Journal of Solid State Chemistry 183 (2010) 636–642

Contents lists available at ScienceDirect

Journal of Solid State Chemistry

journal homepage: www.elsevier.com/locate/jssc

Synthesis and structural characterization of Al_4SiC_4-homeotypic aluminum silicon oxycarbide, $[Al_{4.4}Si_{0.6}][O_{1.0}C_{2.0}]C$

Motoaki Kaga [a], Tomoyuki Iwata [a], Hiromi Nakano [b], Koichiro Fukuda [a,*]

[a] Department of Environmental and Materials Engineering, Nagoya Institute of Technology, Nagoya 466-8555, Japan
[b] Cooperative Research Facility Center, Toyohashi University of Technology, Toyohashi 441-8580, Japan

ARTICLE INFO

Article history:
Received 21 September 2009
Received in revised form
25 December 2009
Accepted 9 January 2010
Available online 18 January 2010

Keywords:
Crystal structure
Powder diffraction
Rietveld method
New material
Aluminum silicon oxycarbide
Al_4SiC_4

ABSTRACT

A new quaternary layered oxycarbide, $[Al_{4.39(5)}Si_{0.61(5)}]_{\Sigma 5}[O_{1.00(2)}C_{2.00(2)}]_{\Sigma 3}C$, has been synthesized and characterized by X-ray powder diffraction, transmission electron microscopy and energy dispersive X-ray spectroscopy (EDX). The title compound was found to be hexagonal with space group $P6_3/mmc$, $Z=2$, and unit-cell dimensions $a=0.32783(1)$ nm, $c=2.16674(7)$ nm and $V=0.20167(1)$ nm^3. The atom ratios Al:Si were determined by EDX, and the initial structural model was derived by the direct methods. The final structural model showed the positional disordering of one of the three types of Al/Si sites. The maximum-entropy methods-based pattern fitting (MPF) method was used to confirm the validity of the split-atom model, in which conventional structure bias caused by assuming intensity partitioning was minimized. The reliability indices calculated from the MPF were $R_{wp}=3.73\%$ ($S=1.20$), $R_p=2.94\%$, $R_B=1.04\%$ and $R_F=0.81\%$. The crystal was an inversion twin. Each twin-related individual was isostructural with Al_4SiC_4 (space group $P6_3mc$, $Z=2$).

1. Introduction

In the Al–Si–C system, there are five types of ternary carbides reported so far; they are Al_8SiC_7, Al_4SiC_4, $Al_4Si_2C_5$, $Al_4Si_3C_6$ and $Al_4Si_4C_7$ with decreasing Al/Si ratio [1–5]. These carbides have the characteristics of layered structures consisting of two types of layers. One is an $[(Al,Si)_4C_4]$ unit layer (A), which is composed of an $[(Al,Si)_2C_2]$ double layer of $(Al,Si)C_4$ tetrahedra surrounded by two $[(Al,Si)C_2]$ single layers of $(Al,Si)C_4$ tetrahedra. The other is an $[(Al,Si)C_2]$ single layer (B) of $(Al,Si)C_4$ tetrahedra. The crystal structures of Al_4SiC_4 and $Al_4Si_2C_5$ (Fig. 1) have been determined by single crystal X-ray diffraction method [3]. The structure of Al_4SiC_4 (space group $P6_3mc$, $Z=2$) is built up of alternately stacking two types of layers with the sequence of $\langle ABAB \rangle$ [6]. For the rhombohedral lattice of $Al_4Si_2C_5$ ($R\bar{3}m$, $Z=3$), the stacking sequence is $\langle BABBABBAB \rangle$ [6]. Although the crystal structures of the other ternary carbides are still not elucidated, they must be also made up of the combinations of A and B layers. The most probable minimum stacking sequences are $\langle ABA \rangle$ for Al_8SiC_7, $\langle BABB \rangle$ for $Al_4Si_3C_6$ and $\langle BBABB \rangle$ for $Al_4Si_4C_7$ [1,6].

Recently, a certain amount of oxygen atoms has been found to readily dissolve into the C sites of both A- and B-type layers, leading to the formation of a new quaternary compound in the Al–Si–O–C system [6]. The monoclinic structure (space group $C2/m$) of the new compound, $[Al_{16.8}Si_{1.2}][O_{3.0}C_{5.0}]C_6$, has been found to be composed of the two A-type $[(Al,Si)_4(O,C)_4]$ unit layers separated by the B-type $[(Al,Si)(O,C)_2]$ single layer with the sequence of $\langle ABA \rangle$, which is comparable to the layer stacking sequence in Al_8SiC_7. The compound is homeotypic to Al_8SiC_7 and therefore regarded as a carbide solid solution rather than an oxycarbide compound. The general formula of the solid solution has been expressed by $Al_{18-x}Si_xO_yC_{14-y}$, where x- and y-values were, respectively, 1.2 and 3.0. The crystal structure of $[Al_{16.8}Si_{1.2}][O_{3.0}C_{5.0}]C_6$ has been satisfactorily expressed by the split-atom model (space group $C2/m$), in which two of the five types of Al/Si sites were positionally disordered. The disordered structure has been regarded as a statistical average of the two twin-related structural configurations with the low-symmetry subgroup Cm. Because the high and low symmetry structures are of the same Bravais lattice but have different point group symmetries, the twinning is by merohedry [7]. The other new types of quaternary oxycarbides are expected to form when the C atoms of the other ternary carbides such as Al_4SiC_4 were partially replaced by O atoms.

Recent advances in the field of crystal-structure analysis from X-ray powder diffraction (XRPD) data have enabled us to investigate unknown structures as well as complex structures, including positional disordering of atoms. To begin with initial structural models are required, which may be determined by, for example, direct methods [8]. The structural parameters are subsequently refined using the Rietveld method [9]. A combined use of the Rietveld method, the maximum-entropy method (MEM) [10] and the

* Corresponding author.
E-mail address: fukuda.koichiro@nitech.ac.jp (K. Fukuda).

0022-4596/$ - see front matter © 2010 Elsevier Inc. All rights reserved.
doi:10.1016/j.jssc.2010.01.012

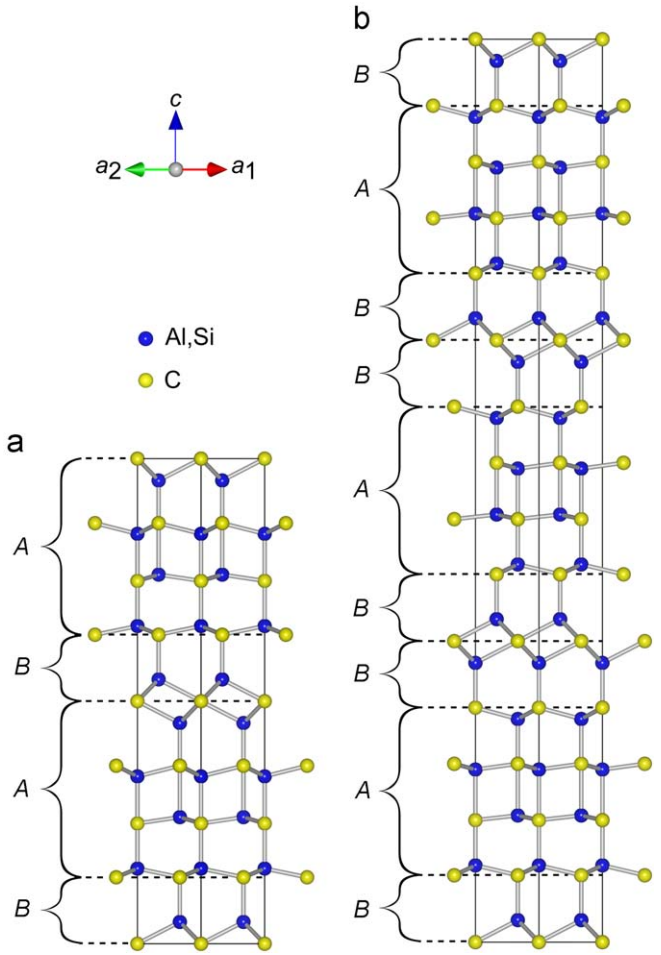

Fig. 1. Atomic configurations in (a) Al_4SiC_4 and (b) $Al_4Si_2C_5$, showing the crystal structures being made up of two types of layers *A* and *B* [3].

MEM-based pattern fitting (MPF) method [11] has enabled us to disclose new structural details. MEM is capable of estimating structure factors of unobserved reflections and improving those of overlapped reflections, which give MEM advantages over the classical Fourier method. However, the Rietveld method and MEM have a drawback in determining the electron-density distributions (EDD) because the observed structure factors, F_o(Rietveld), are biased toward the structural model assuming intensity partitioning. On the other hand, the MPF method can minimize the structural bias. Thus, the MEM and MPF analyses are alternately repeated (REMEDY cycle) until the reliability indices reach minima. Crystal structures can be seen clearly from EDD determined by MPF.

In the present study, we have discovered a new quaternary oxycarbide in the Al–Si–O–C system. The layer stacking sequence was comparable to that of Al_4SiC_4. We determined the initial structural model from XRPD data using direct methods and further modified it into a split-atom model, in which one of the three types of Al/Si sites was positionally disordered. The crystal was most probably an inversion twin with nearly the same twin fraction.

2. Experimental

2.1. Synthesis

We initially tried to synthesize the samples exclusively consisting of Al_4SiC_4 using the stoichiometric mixture of reagent-grade chemicals of Al_4C_3 (98%, Mitsuwa Chemical Co., Ltd., Kanagawa, Japan) and SiC (99%, KCL Co., Ltd., Saitama, Japan). However, an excess amount of Al_4C_3 was necessarily required for the preparation of a single phase, which was obtained by the following procedure. The reagent-grade chemicals of Al_4C_3 and SiC were mixed in molar ratios of Al_4C_3:SiC=1.5:1, corresponding to Al:Si=0.86:0.14. The well-mixed chemicals were pressed into pellets ($\varnothing$ 15 mm × 10 mm), heated at 2073 K for 1 h in inert gas atmosphere of Ar, followed by cooling to ambient temperature by cutting furnace power. The reaction product was a slightly sintered polycrystalline material.

2.2. Characterization

The sample was finely ground to obtain powder specimen and introduced into a 0.4 mm diameter glass capillary tube of internal diameter approximately 0.3 mm. The XRPD intensities were collected on a diffractometer (X'Pert PRO MPD, PANalytical B.V., Almelo, The Netherlands) equipped with a high speed detector in Debye–Scherrer geometry using Cu$K\alpha$ radiation (45 kV, 40 mA) in a 2θ range from 2.0042° to 136.0035° (an accuracy in 2θ of $\pm$0.0001°). Other experimental conditions were: continuous scan, total of 15 679 datapoints and total experimental time of 35.5 h. No preferred orientation could be seen in the diffraction pattern which was collected with the specimen rotating. We corrected the X-ray absorption using the μr value (μ: linear absorption coefficient; r: sample radius) of the sample and capillary tube, which was determined by the transmittance of direct incident beam. The structure data were standardized according to rules formulated by Parthé and Gelato [12] using the computer program STRUCTURE TIDY [13]. The crystal-structure models and equidensity isosurfaces of EDD were visualized with the computer program VESTA [14].

The powder specimen was also examined using a transmission electron microscope (JEM 2100F, JEOL Ltd., Tokyo, Japan) operated at 200 kV and equipped with an energy dispersive X-ray analyzer (EDX; JED-2300, JEOL Ltd., Tokyo, Japan). The powder particles were deposited with ethyl alcohol on a copper grid. Selected area electron diffraction (SAED) patterns and corresponding lattice images were obtained. A chemical analysis was made to quantitatively determine the atom ratios Al:Si. The correction was made by the ZAF routines.

3. Results and discussion

3.1. Unit cell and chemical composition

The SAED pattern was successfully indexed with a hexagonal unit cell with dimensions of $a \approx 0.33$ nm and $c \approx 2.2$ nm (Fig. 2). The corresponding lattice image strongly suggests that the crystal is characterized by a layered structure with the periodicity of about 2.2 nm along the c axis. The EDX spectrum showed the existence of a small amount of O atoms within the crystal lattice (Fig. 3). The O atoms might be originated from the impurities of Ar gas and introduced into the sample during the crystal growth process. The atom ratios Al:Si were determined by measuring one point for each of 10 crystal fragments to be 0.88(1):0.12(1), where the numbers in parentheses indicate standard deviations. These ratios were equivalent to those of the starting mixture.

The unit-cell parameters as well as the integrated intensities were refined by the Le Bail method [15] using the computer program RIETAN-FP [16]. The refined unit-cell dimensions were a=0.328003(5) nm and c=2.16809(3), which could successfully index all the observed reflections in the experimental diffraction pattern. The observed diffraction peaks were examined to

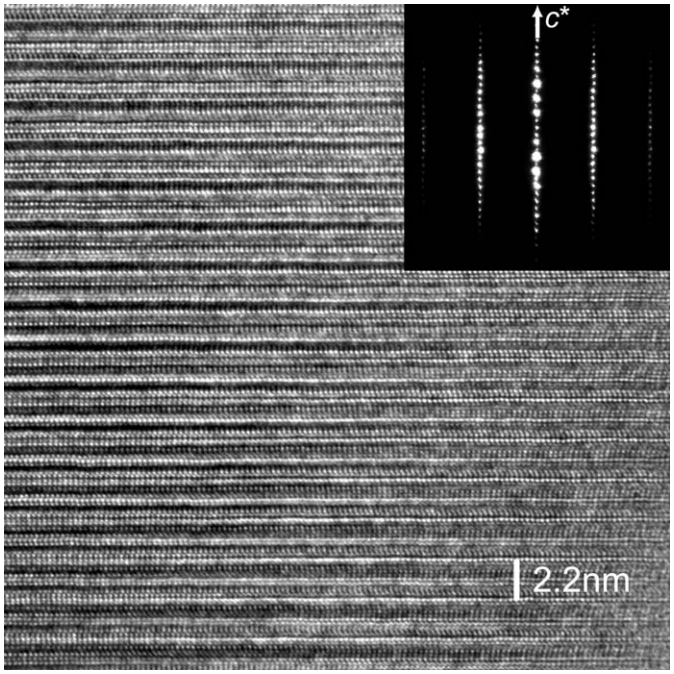

Fig. 2. Selected-area electron diffraction pattern and corresponding lattice image. Incident beam almost parallel to the *a* axis.

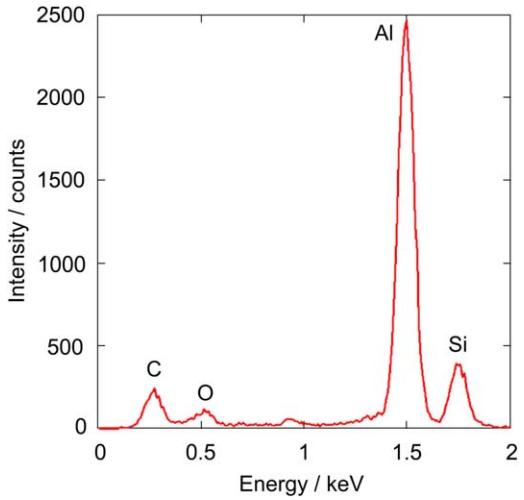

Fig. 3. Identification of the presence of Al, Si, O and C in the compound. EDX spectrum.

determine the presence or absence of reflections. Systematic absences $l \neq 2n$ for $hh\bar{2}hl$ and $l \neq 2n$ for $000l$ reflections were found, which implies that possible space groups are $P31c$, $P\bar{3}1c$, $P6_3mc$, $P\bar{6}2c$ and $P6_3/mmc$.

The intensity distributions of XRPD pattern as well as the refined unit-cell dimensions were compatible with those of Al_4SiC_4 (V=0.20160 nm^3 and Z=2) [3]. Because the unit-cell content of this compound is [8Al 2Si 8C] (Al+Si=10), that of the new one (V=0.20201 nm^3) must be [8.8Al 1.2Si 8(O+C)] (Al:Si=0.88:0.12, Al+Si=10), assuming that the O atoms exclusively occupy the C sites. The crystal structure of the present oxycarbide must be closely related to that of Al_4SiC_4 (space group $P6_3mc$). However, the incorporation of O atoms into the C sites can modify the crystal structure. Thus, attempts were made to derive the crystal-structure models using the direct methods based on the possible space groups.

3.2. Initial structural model

Because the atomic scattering factors for Al and Si are almost the same and the oxygen concentration is relatively low, we used a unit-cell content with [10Al 8C] as input data for the search of a crystal-structure model. All of the possible space groups were tested using the EXPO2004 package [8] for crystal structure determination. The individual integrated intensities that were refined by the Le Bail method were used for the direct methods. A promising structural model with a minimum reliability index R_F of 17.9% was found with the space group $P6_3/mmc$ (centrosymmetric) in a default run of the program. There were six independent sites in the unit cell; three Al/Si sites were located at the Wyckoff position 4*e* (Al/Si1), 4*f* (Al/Si2) and 2*c* (Al/Si3), and three O/C sites were located at 2*a* (O/C1), 2*b* (O/C2) and 4*f* (O/C3).

The structural parameters of all atoms were subsequently refined by the Rietveld method using the computer program RIETAN-FP using the profile intensity data in the 2θ range of 6.0065–130.7561°. A Legendre polynomial was fitted to background intensities with 12 adjustable parameters. The pseudo-Voigt function [17] was used to fit the peak profile. The Si and Al atoms were assumed to be randomly distributed over the same sites in the crystal structure, although there might be the site preference of these atoms. The occupancies of O and C atoms in each O/C site were refined without any constraints. The isotropic displacement (B) parameters for O and C atoms were constrained to be equal. Because the site occupancies (g) and corresponding B parameters were strongly correlated, they were refined alternately in successive least-squares cycles. The O atoms preferentially occupied the O/C2 and O/C3 sites, the g(O)-values of which were 0.34(3) and 0.33(2), respectively. Because of the absence of O atoms at O/C1 site, the O/C1, O/C2 and O/C3 sites were relabeled C, O/C1 and O/C2, respectively. The refinement, however, resulted in the relatively large B parameters for the Al/Si3 site (B(Al/Si3)=2.5(1)$\times 10^{-2}$ nm^2) with the less satisfactory reliability (R) indices [18] of R_{wp}=4.43% (S=R_{wp}/R_e=1.43), R_p=3.39%, R_B=4.77% and R_F=3.32%. These findings promoted us to build split-atom models for Al/Si3.

3.3. Split-atom model

In the split-atom model, the site symmetry of Al/Si3 was decreased from 2*c* (point symmetry $\bar{6}m2$) to 4*f* (3*m*) with the g(Al/Si3) value being reduced to 1/2. The subsequent Rietveld refinement resulted in satisfactory B parameters for all the sites with R indices of R_{wp}=3.79% (S=1.22), R_p=2.97%, R_B=3.34% and R_F=2.33%, indicating that the disordered arrangement of Al/Si3 site can be represented adequately with the split-atom model in Fig. 4. The separation distance of atoms in the Al/Si3 site was 0.0516(3) nm. Crystal data are given in Table 1, and ;the final atomic positional and B parameters are given in Table 2. The chemical composition was found to be $Al_{4.39(5)}Si_{0.61(5)}O_{1.00(2)}C_{3.00(2)}$, with the chemical formula of $[Al_{4.39(5)}Si_{0.61(5)}]_{\Sigma 5}[O_{1.00(2)}C_{2.00(2)}]_{\Sigma 3}C$ (space group $P6_3/mmc$, Z=2).

The MPF method was subsequently used to confirm the validity of the split-atom model. After two REMEDY cycles, R_{wp}, S, R_p, R_B and R_F decreased to 3.73%, 1.20, 2.94%, 1.04% and 0.81%, respectively. Subtle EDD changes as revealed by MPF significantly improve the R_B and R_F indices. The decreases in R indices demonstrate that the present disordered structure can be seen more clearly from EDD rather than from the conventional structural parameters reported in Table 2. Observed, calculated, and difference XRPD patterns for the MPF are plotted in Fig. 5. The EDD determined by MPF are in reasonably good agreement with the atom arrangements. For example, the three-dimensional EDD at the Al/Si3 site was elongated along the *c* axis,

the equidensity isosurfaces of which are in harmony with the atom arrangements (Fig. 6). We therefore concluded that, as long as the crystal structure was expressed by a structural model, the present split-atom model would be satisfactory.

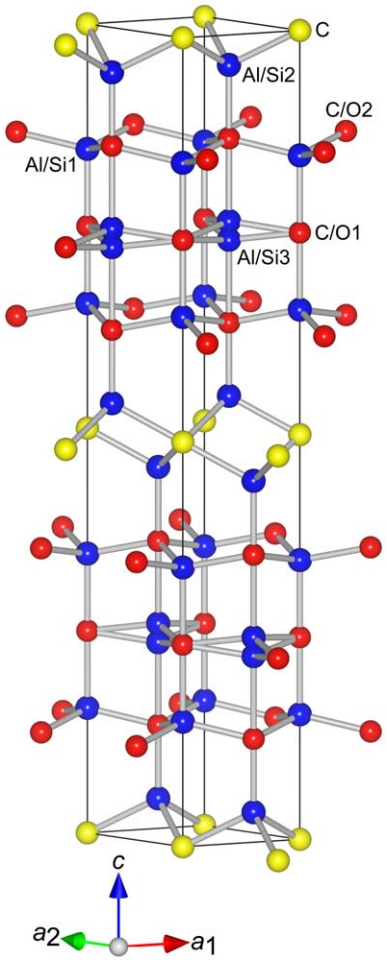

Fig. 4. Crystal structure of $[Al_{4.4}Si_{0.6}][O_{1.0}C_{2.0}]C$. Space group $P6_3/mmc$.

3.4. Description of twinning structure and crystal structure

The disordered structure can be regarded as a statistical average of the two twin-related structural configurations with the low-symmetry subgroup $P6_3mc$. When the mirror plane perpendicular to the c axis is removed from the space group $P6_3/mmc$, the resulting space group is $P6_3mc$, with a center of symmetry being lost concomitantly. The two structural configurations as shown in Fig. 7 are therefore related not only by a pseudo-symmetry mirror plane but also by a pseudo-symmetry inversion. Thus, the crystal must be an inversion twin. Actually we observed using TEM two interpenetrating domains (Fig. 8). The lattice fringes around the domain boundary showed translational misfit of approximately 0.8 nm along the common c axis. We refined the crystal structure using the space group $P6_3mc$ to obtain an unsatisfactory result; the resulting reliability indices were

Table 1
Crystal data for $[Al_{4.4}Si_{0.6}][O_{1.0}C_{2.0}]C$.

Chemical composition	$Al_{4.39(5)}Si_{0.61(5)}O_{1.00(2)}C_{3.00(2)}$
Space group	$P6_3/mmc$
a (nm)	0.32783(1)
c (nm)	2.16674(7)
V (nm^3)	0.20167(1)
Z	2
D_x (Mgm^{-3})	3.090

Table 2
Structural parameters for $[Al_{4.4}Si_{0.6}][O_{1.0}C_{2.0}]C$[a].

Site	Wyckoff position	g	x	y	z	$100 \times B$ (nm^2)
Al/Si1	4*e*	1	0	0	0.15466(4)	0.98(2)
Al/Si2	4*f*	1	1/3	2/3	0.04529(4)	1.16(2)
Al/Si3	4*f*	1/2	1/3	2/3	0.23810(8)	0.78(3)
C	2*a*	1	0	0	0	1.37 (3)
O/C1	2*b*	1	0	0	1/4	1.37
O/C2	4*f*	1	1/3	2/3	0.13529(8)	1.37

[a] Site occupancies: O/C1: 62.6(9)% C and 37.4(9)% O; O/C2: 68.5(7)% C and 31.5(7)% O.

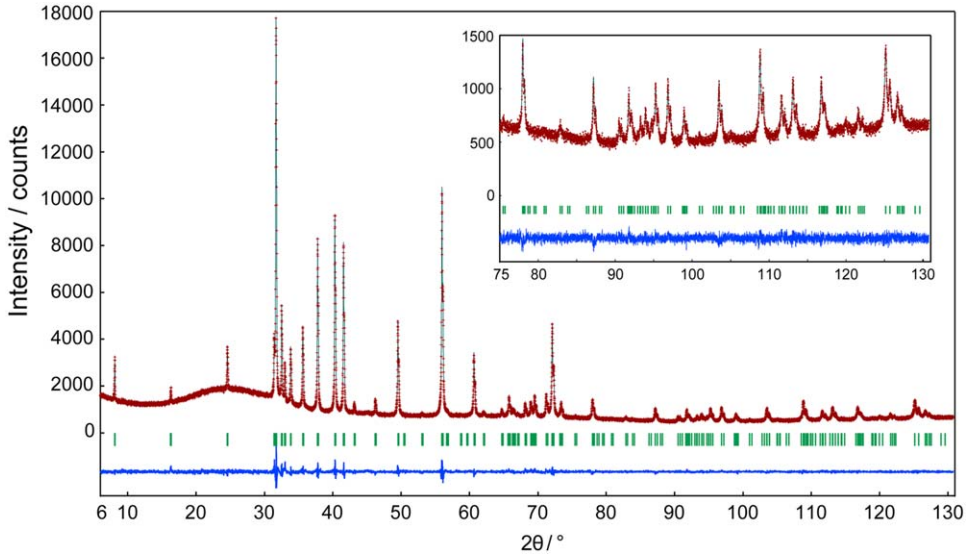

Fig. 5. Comparison of the observed diffraction pattern of $[Al_{4.4}Si_{0.6}][O_{1.0}C_{2.0}]C$ (symbol: +) with the corresponding calculated pattern (upper solid line). The difference curve is shown in the lower part of the diagram. Vertical bars indicate the positions of Bragg reflections.

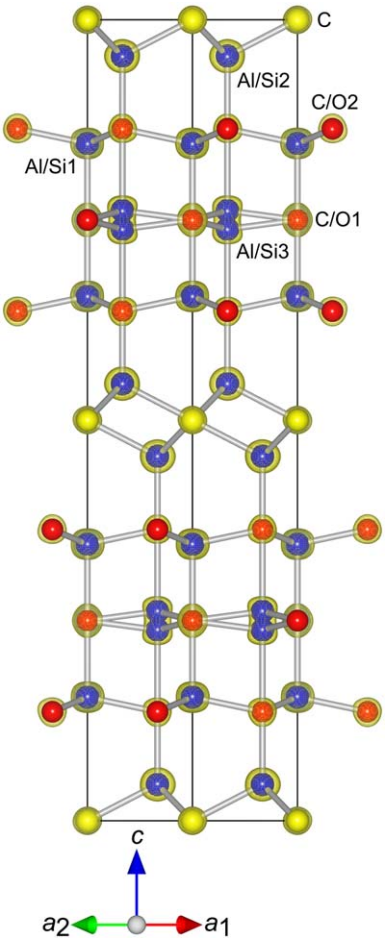

Fig. 6. Three-dimensional electron density distribution determined by MPF with the split-atom model viewed along [110]. Isosurfaces expressed in wireframe style for an equidensity level of 0.004 nm^{-3}.

R_{wp}=4.36% (S=1.41), R_p=3.35%, R_B=5.38% and R_F=4.24%, which are much higher than those of the Rietveld refinement with the space group $P6_3/mmc$.

The layer stacking sequences within the unit cell are different between the two structural configurations related by a pseudo-symmetry inversion; one is $\langle ABAB \rangle$ along the c axis [Fig. 7(a)] and the other is $\langle BABA \rangle$ [Fig. 7(b)]. Thus the former layer stacking sequence is, with respect to the latter, displaced along the c direction by 0.790 nm, which corresponds to the A-type layer thickness. These magnitude and direction of displacement are in agreement with those of the misfit between the two interpenetrating domains (Fig. 8). Accordingly, the two domains must be related by merohedral twinning, the twin individuals of which are related by the pseudo-symmetry inversion. The dimensions of twin domains would be within the coherence range of X-rays and also the domain ratio should be almost 0.5:0.5, hence the crystal structure has been successfully represented by the split-atom model. A similar split-atom model has been reported for α'-Sr_2SiO_4 (space group $Pmnb$), the structural model of which was considered to be a statistical average of two structural configurations with $P2_1/n$ symmetry [19]. The present twin boundaries are probably formed during crystal growth or phase transformations. Provided the phase transformation occurred during cooling from 2073 K to ambient temperature, the space group would change from $P6_3/mmc$ of the high temperature phase to $P6_3mc$ of the low temperature phase. The more detailed examination would be necessary for the present domain boundaries to determine the origin of the twinning (Fig. 8).

In Table 3, only (Al,Si)–(O,C) bonds belonging to one of the two twin-related orientations are reported, excluding possible bonds between atoms of different orientation states. The Al and Si atoms are tetrahedrally coordinated by O and/or C atoms with the mean (Al,Si)–(O,C) distance of 0.201 nm, which is comparable to the mean (Al,Si)–(O,C) distances of the $[(Al,Si)(O,C)_4]$ polyhedra in $[Al_{16.8}Si_{1.2}][O_{3.0}C_{5.0}]C_6$ (0.205 nm) and Al_4SiC_4 (0.202 nm). There is a possibility of site preference of Al and Si in the Al/Si sites. Hence we tried to extract the information on site preference from the (Al,Si)–(O,C) distances; however, the obtained results could not be regarded as significant. Because the mean interatomic distance as well as the atomic configurations of $[Al_{4.4}Si_{0.6}][O_{1.0}C_{2.0}]C$ compares well with those of Al_4SiC_4, this oxycarbide can be regarded as, from a structural point of view, a carbide solid solution in which 25.1% C sites were occupied by O atoms rather than an oxycarbide compound [6]. The general formula of the solid solution is expressed by $[Al_{5-x}Si_x][O_yC_{4-y}]$, where x- and y-values are, respectively, 0.6 and 1.0 for the sample. Further work is necessary to confirm the real existence of oxygen-free end member of Al_4SiC_4 (x=1 and y=0).

In the system Al–Si–O–C, the authors have discovered and structurally characterized the two types of new oxycarbides, Al_8SiC_7-homeotypic $[Al_{16.8}Si_{1.2}][O_{3.0}C_{5.0}]C_6$ in a previous study [6] and Al_4SiC_4-homeotypic $[Al_{4.4}Si_{0.6}][O_{1.0}C_{2.0}]C$ in the present study. These oxycarbides have the characteristics of the layered structures, hence the general formula is expressed by

$$(Al,Si)_{4l+m}(O,C)_{3l+m} \quad (1)$$

where l and m are, respectively, the numbers of A-type $[(Al,Si)_4(O,C)_4]$ unit layer and B-type $[(Al,Si)(O,C)_2]$ single layer of the minimum stacking sequence. The (l, m) values are (2, 1) for $[Al_{16.8}Si_{1.2}][O_{3.0}C_{5.0}]C_6$ and (1, 1) for $[Al_{4.4}Si_{0.6}][O_{1.0}C_{2.0}]C$. In a similar manner, new types of oxycarbides are expected to form when O atoms were dissolved into the other ternary carbides than Al_8SiC_7 and Al_4SiC_4. Because the minimum stacking sequences are $\langle BAB \rangle$ for $Al_4Si_2C_5$, $\langle BABB \rangle$ for $Al_4Si_3C_6$ and $\langle BBABB \rangle$ for $Al_4Si_4C_7$, the corresponding (l, m) values of the general formula (1) are, respectively, (1, 2), (1, 3) and (1, 4).

4. Conclusion

We have successfully synthesized a new quaternary layered oxycarbide $[Al_{4.4}Si_{0.6}][O_{1.0}C_{2.0}]C$. The crystal structure was satisfactorily represented by the split-atom model with the space group $P6_3/mmc$ (centrosymmetric). The crystal was composed of the two twin-related individuals with low-symmetry subgroup $P6_3mc$ (noncentrosymmetric), each of which was isostructural with Al_4SiC_4.

Acknowledgments

Supported by a Grant-in-Aid for Scientific Research (no. 21360322) from the Japan Society for the Promotion of Science. Thanks are due to Mr. I. Yamaji, PANalytical Japan, Spectris Co. Ltd., for his technical assistance in XRPD.

Appendix A. Supplementary material

Supplementary data associated with this article can be found in the online version at doi:10.1016/j.jssc.2010.01.012.

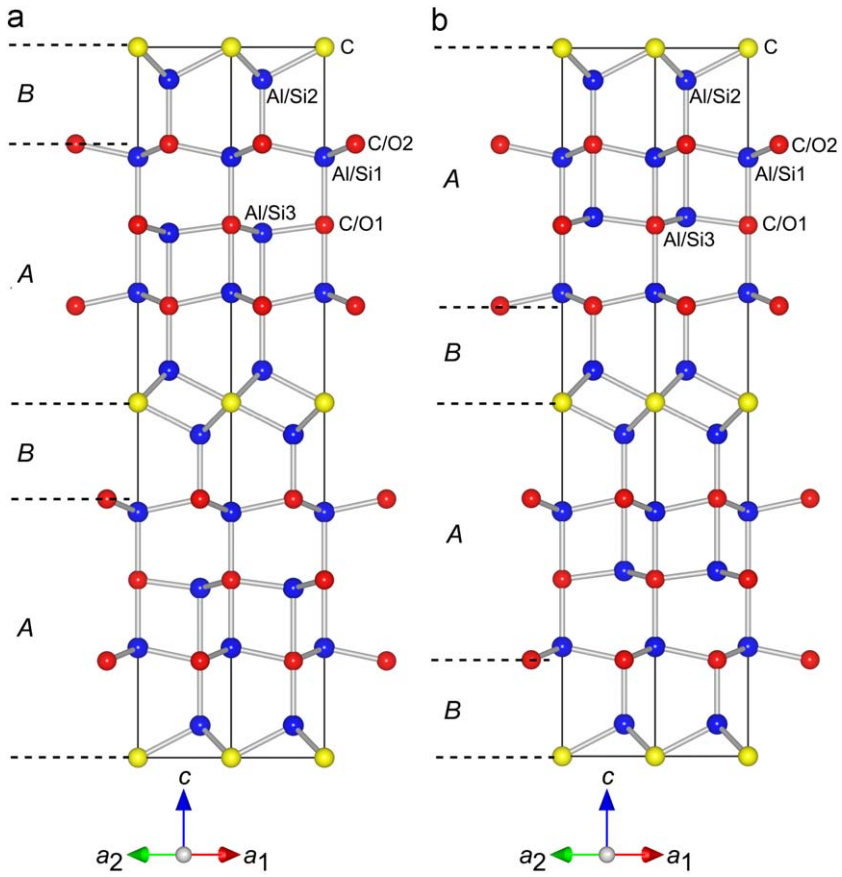

Fig. 7. Crystal structures of the two orientation states of $[Al_{4.4}Si_{0.6}][O_{1.0}C_{2.0}]C$ viewed along [110], showing the crystal structures being made up of two types of layers *A* and *B*. The two structural configurations (a) and (b) are related by the pseudo-symmetry inversion.

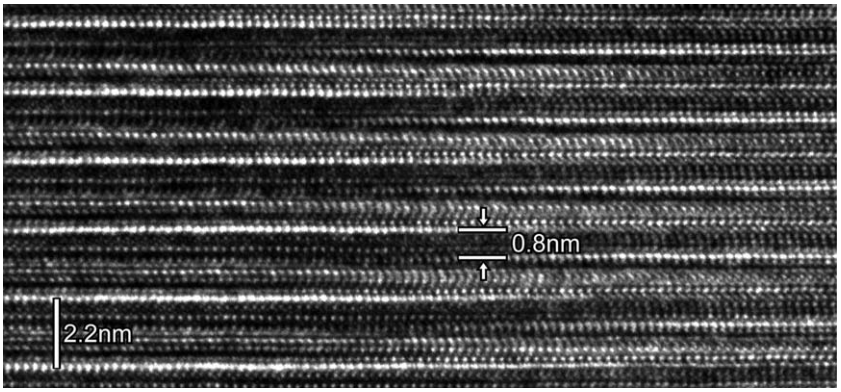

Fig. 8. Lattice images of mutually interpenetrating twin-related domains. Viewed along [100]. The fringes around the domain boundary show translational misfit of approximately 0.8 nm along the *c* direction.

Table 3
Interatomic distances (nm) in $[Al_{4.4}Si_{0.6}][O_{1.0}C_{2.0}]C$.

Al/Si1–O/C2	0.19387(4) × 3
Al/Si1–O/C1	0.20658(8)
〈Al/Si1–C〉	0.197
Al/Si2–O/C2	0.1950(2)
Al/Si2–C	0.21320(4) × 3
〈Al/Si2–O/C〉	0.209
Al/Si3–O/C1	0.19102(2) × 3
Al/Si3–O/C2	0.2228(3)
〈Al/Si3–O/C〉	0.199

References

[1] R.J. Oscroft, P. Korgul, D.P. Thompson, Br. Ceram. Proc. 42 (1989) 33–47.
[2] G.A. Jefeerey, V.Y. Wu, Acta Crystallogr. 20 (1966) 538–547.
[3] Z. Inoue, Y. Inomata, H. Tanaka, H. Kawabata, J. Mater. Sci. 15 (1980) 575–580.
[4] J. Schoennahl, B. Willer, M.J. Daire, Solid State Chem. 52 (1984) 163–173.
[5] B.L. Kidwell, L.L. Oden, R.A. McCune, J. Appl. Crystallogr. 17 (1984) 481–482.
[6] T. Iwata, M. Kaga, H. Nakano, K. Fukuda, J. Solid State Chem. 182 (2009) 2252–2260.
[7] N.G.L. Nord, Jr., in: P.R. Buseck (Ed.), Minerals and Reactions at the Atomic Scale: Transmission Electron Microscopy: Imaging Transformation-Induced Microstructures, Mineralogical Society of America, Washington, DC, USA, 1992, pp. 455–508.
[8] A. Altomare, M.C. Burla, M. Camalli, B. Carrozzini, G.L. Cascarano, C. Giacovazzo, A. Guagliardi, A.G.G. Moliterni, G. Polidori, R. Rizzi, J. Appl. Crystallogr. 32 (1999) 339–340.

[9] H.M. Rietveld, J. Appl. Crystallogr. 2 (1969) 65–71.
[10] M. Takata, E. Nishibori, M. Sakata, Z. Kristallogr. 216 (2001) 71–86.
[11] F. Izumi, S. Kumazawa, T. Ikeda, W.-Z. Hu, A. Yamamoto, K. Oikawa, Mater. Sci. Forum 378–381 (2001) 59–64.
[12] E. Parthé, L.M. Gelato, Acta Crystallogr. A 40 (1984) 169–183.
[13] L.M. Gelato, E. Parthé, J. Appl. Crystallogr. 20 (1987) 139–143.
[14] K. Momma, F. Izumi, J. Appl. Crystallogr. 41 (2008) 653–658.
[15] A. Le Bail, H. Duroy, J.L. Fourquet, Mater. Res. Bull. 23 (1988) 447–452.
[16] F. Izumi, K. Momma, Solid State Phenom. 130 (2007) 15–20.
[17] H. Toraya, J. Appl. Crystallogr. 23 (1990) 485–491.
[18] R.A. Young, in: R.A. Young (Ed.), The Rietveld Method, Oxford University Press, Oxford, UK, 1993, pp. 1–38.
[19] M. Catti, G. Gazzoni, G. Ivaldi, G. Zanin, Acta Crystallogr. B 39 (1983) 674–679.